Infrared contribution to the double-logarithmic small-x asymptotics of structure functions

S. I. Manayenkov and M. G. Ryskin *

Petersburg Nuclear Physics Institute,
Russian Academy of Science,
Gatchina, St.Petersburg district, 188350, Russia

Abstract

The role playing by the "soft" ($k_T < 1$ GeV/c) region in the small-x behaviour of $g_1(x, Q^2)$ and the non-singlet structure function $f_{1,NS}(x, Q^2)$ has been studied with the help of the effective QCD Lagrangian which takes into account the lightest degrees of freedom - the constituent quarks and the π-mesons (Goldstone bosons). It has been shown that the quark-quark interaction due to the pion exchange has a negative coupling g for the isovector component ($I = 1$ in the t-channel) of $f_1(x, Q^2)$ and isosinglet component of $g_1(x, Q^2)$. Here the pion induced interaction changes mainly the normalization of the quark distribution (it decreases $f^{I=1}_{1,NS}(x, Q^2)$ two times at $x < 3 \cdot 10^{-3}$) and changes slightly the effective exponents λ ($f_{1,NS}$, $g_1 \sim x^{-\lambda}$ at $x \to 0$). On the other hand due to a positive value of coupling g the value of λ increases by 15% for the isovector part of $g_1(x, Q^2)$ and up to $\lambda \approx 0.5$ (instead of $\lambda \approx 0.2$ without the pion contribution) for the isoscalar non-singlet structure function $f^{I=0}_{1,NS}(x, Q^2)$.

1 Introduction

The small-x behaviour of the deep inelastic structure functions plays an important role in the precise description of the quark densities. As it is known [1], [2], [3], [4], [5] one cannot use the conventional DGLAP [6], [7], [8] evolution equations to study the non-singlet structure functions at very low x ($x \ll 1$) or the singlet spin-dependent structure functions. Instead of the usual k_T ordering ($k^2_{i+1,T} \ll k^2_{i,T}$), here the leading logarithmic contribution comes from the region of

$$k^2_{i+1,T} \ll \beta_{i+1} k^2_{i,T} / \beta_i \ . \tag{1}$$

In (1) $k_{i,T}$ and β_i are the transverse momentum and the longitudinal momentum fraction of the quark with four-momentum k_i (see Fig. 1). This means that for small x when $\beta_{i+1}/\beta_i \gg 1$ we can face with the inverse ordering of transverse momenta ($k^2_{i+1,T} \gg k^2_{i,T}$). Even more, not excluded that in the middle of the evolution chain the values of $k_{i,T}$ become close to the infrared region ($k_{i,T} \sim \mu$) again (as at the beginning of the evolution).

In the framework of the double-logarithmic (DL) approximation with a constant QCD coupling (α_s fixed) a convenient way to calculate the amplitude (or the structure

*The work is supported by the Grant INTAS-93-283-ext

function) in this limit ($x \ll 1$) is to use the Kirshner-Lipatov infrared evolution equation [9], i.e. to consider the evolution of parton distributions with respect to the infrared cut off parameter μ [1]. Using this method the small-x asymptotics of the non-singlet unpolarized and polarized structure functions have been studied [3], [4]

$$
\begin{aligned}
f_1^{NS}(x, Q^2) &\sim x^{-\omega^{(+)}}, \\
g_1^{NS}(x, Q^2) &\sim x^{-\omega^{(-)}}
\end{aligned}
\tag{2}
$$

where

$$
\omega^{(+)} = \sqrt{2C_F \alpha_s/\pi}, \quad \omega^{(-)} = 1.04\omega^{(+)} . \tag{3}
$$

For the colour group $SU_c(N)$ the colour factor in (3) $C_F = (N^2-1)/(2N)$. We consider the case $N = 3$ only. Unfortunately, it is not clear which value of α_s one has to put in (2). Of course it should be somewhere between $\alpha_s(\mu^2)$ and $\alpha_s(Q^2/x)$, but the interval is too large to make a definite prediction. For the case of the unpolarized distribution $f_1(x, Q^2)$, where the non-ladder Feynman diagrams do not contribute within the DL approximation the linear evolution equation with the ordering (1) and the running coupling $\alpha_s(q^2) = 4\pi/[b\ln(q^2/\Lambda^2)]$ can be solved explicitly [10]. In the small x limit $f_1(x, Q^2) \sim x^{-\lambda}$, where the value of λ depends on the cut-off parameter μ and in the extreme case $\mu = \Lambda$ the power $\lambda = 2C_F/b$.

However it is hard to believe that the DL approximation of QCD is still valid at k_T close to the infrared region when the coupling $\alpha_s(k_T^2) > 1$. The best we can do at the moment is to consider the perturbative QCD evolution in the region of rather large transverse momenta (say, $k_T > 1$ GeV/c) and to use the effective Lagrangian of QCD, which takes into account only the lightest degrees of freedom (light constituent quarks with mass $M \approx 350$ MeV and the Goldstone pseudoscalar mesons π^+, π^0, π^-) for small k_T (< 1 GeV/c). As it has been shown in [11], starting from the simplest $SU(6)$ wave function of a nucleon (i.e. from the additive quark model) at low virtualities ($Q^2 \sim M^2$) the leading logarithmic evolution, described in the framework of the effective Lagrangian, gives us (at $Q^2 \sim 1$ (GeV/c)^2) a reasonable explanation of the two important effects simultaneously: the experimentally observed "spin crisis" ($\Delta\Sigma = \Delta u + \Delta d + \Delta s \approx 0.3 < 1$) and the violation of the Gottfried sum rule $\int_0^1 [F_2^p(x) - F_2^n(x)]dx/x = 0.24 \pm 0.016 < 1/3$ measured in [12]. This gives us a hope that the same effective Lagrangian would provide reasonable continuation into the small-k_T region in our case (small-x behaviour of the DL structure functions) also. It is interesting to note that the emission of pions (at low-k_T) diminishes the asymptotic value of the unpolarized quark density $f_{1,NS}^{I=1}(x, Q^2)$ with the t-channel isospin $I = 1$ but increases (almost by 3 times) the spin-dependent distribution $g_{1,NS}^{I=1}(x, Q^2)$ at $x \ll 1$. Not excluded that it is the fact which may explain the large difference between the values of the proton and neutron structure functions $g_1^p(x, Q^2) - g_1^n(x, Q^2)$ at rather small $x \sim 0.01$ measured by the SMC [13]. At the same time in the singlet channel the quark-quark pion induced interaction diminishes the small-x asymptotics of the singlet structure function $g_{1,S}(x, Q^2)$.

In Sect. 2 we remind the form of the double-logarithmic evolution equation for singlet and non-singlet structure functions with the running coupling α_s and the effective QCD

[1] To be more precise - the evolution over the $\ln \mu^2$, under the condition: $k_{iT} \geq \mu$.

Lagrangian. In Sect. 3 the numerical calculations of the structure functions at small x are discussed. We summarize our results in Sect. 4. Analytical formulae for the non-singlet structure functions taking into account both the nonperturbative QCD and pion exchange contributions are presented in Appendix.

2 Double-logarithmic evolution

2.1 Non-singlet structure functions

First of all let us define what we call here the non-singlet structure function $f_{1,NS}(x,Q^2)$ or $g_{1,NS}(x,Q^2)$. In the case of pure QCD the non-singlet component corresponds to the evolution of the initial quark (Fig. 1), where one has only one fermion line, and no any new quark-antiquark pair was produced during the evolution. As the gluon emission does not change the quark flavour the sort of the final (upper in Fig. 1) quark, which absorbs the heavy photon, is the same as the sort of the initial quark. Taking into account the pion emission one faces with a new possibility: due to the isospin of the pion (I=1) the flavour of the t-channel (vertical) quark may be changed. Thus we have to consider separately the t-channel isosinglet and isovector sets of the diagrams, i.e. there are two types of the non-singlet structure functions - with the isospin $I=0$ (say, $f_{1,NS}^{I=0}(x,Q^2)$) and with $I=1$ ($f_{1,NS}^{I=1}(x,Q^2)$). Only the baryon charge does conserve now during the non-singlet evolution.

Owing to the linearity of the evolution equation the final structure function can be written as the sum of the singlet and non-singlet components. In the singlet case one deals with the system of two equations (for quarks and gluons). So there are two eigenfunctions and we have to choose its relative contribution (i.e. the coefficients in front of these functions) starting from the conditions that these two singlet components should reproduce the initial gluon distribution $G(x,Q^2)$ and the first derivative $\partial G(x,Q^2)/\partial \ln Q^2$ at $Q^2=Q_0^2$. Then one has to add the non-singlet components, corresponding to the quark (and separately antiquark) evolution with the t-channel isospin $I=0$ (and/or 1) in order to reproduce the initial quark (antiquark) distribution at $Q^2=Q_0^2$. Here one has to take into account that some fermion component (with the equal quark and antiquark densities) are already contained in the singlet structure functions. Thus, even having no antiquarks in the initial states, one has to add the antiquark non-singlet component in order to cancel the antiquark contribution coming from the singlet part.

Below we will use the double-logarithmic evolution equation in the integral form as it has been done in [3]. First such an equation has been considered for the case of QED (the $e^+e^-\to\mu^+\mu^-$ annihilation at small momentum transfer) in [1], [2]. It is convenient to introduce the quark-quark amplitude $A(t,\beta)$, which satisfies the equation [3]

$$A(t,\beta)=\int_\beta^1\frac{d\beta'}{\beta'}\int_{\mu^2}^{t_m}\frac{dt'}{t'}G(t_m)A(t',\beta')+A_0(t,\beta) \tag{4}$$

(where the upper limit of the t' integral is $t_m=t\beta'/\beta$) and to write the non-singlet structure function as

$$f_{1,NS}(x,Q^2)=e_q^2\Big[\delta(x-1)+\int_{\mu^2}^{S_m}A(t,\tilde\beta)\frac{dt}{t}\Big] \tag{5}$$

with $\tilde{\beta} = x + t/s$ and $S_m = Q^2/(4x)$. In (5) e_q is the fractional electrical charge of a quark. We have applied the Sudakov parametrization [14] for k

$$k = -\alpha q' + \beta p + k_T \tag{6}$$

where $q'_\mu = q_\mu - p_\mu q^2/2(pq)$, $(q')^2 \approx 0$, $t = -k_T^2 > 0$, $s = 2(pq)$ and the analogous parametrization for k' (and for k_j in Fig. 1 with parameters α_j and β_j). The unhomogeneous term reads

$$A_0(t,\beta) = \frac{C_F}{2\pi}\alpha_s(t/\beta)\ . \tag{7}$$

.

For the case of the perturbative QCD equations (4), (5) have been discussed in detail in [3]. Eq. (4) contains two logarithmic integrals. The first one is over β' with the natural limits from β to 1 and the second integration over $t' = |k'_T|^2$ runs from the infrared cut-off μ^2. The upper limit

$$t_m = t\beta'/\beta \tag{8}$$

is controlled by the condition $|k^2_{i,||}| \ll |k^2_{i,T}|$ (i.e. the virtuality of the t-channel line should be very close to the transverse momentum square transferred through this line. In other case one looses one logarithmic integration dk_T^2/k_T^2). As it has been shown in [3] the argument of the running QCD coupling is also given by the value of t_m so for the gluon emission $G(t_m) = C_F\alpha_s(t_m)/2\pi$. It is nothing else but the value of the Altarelli-Parisi splitting kernel at $z \to 0$, i.e. near the leading ($j = 0$) singularity which gives us the double-logarithmic contribution.

The final loop gives only one logarithm [2] and we have written this last integration separately in relation (5). The upper limit is $S_m = |k_{T,max}|^2 = s/4$. Of course, one can use this double-logarithmic approximation in the framework of the perturbative QCD at small distances only, i.e. when the transverse momentum of the emitted gluons is large enough, say, $|k_{g,T}| > 1$ GeV/c. For a smaller k_T we shall use the effective Lagrangian which takes into account the lightest degrees of freedom - the constituent quarks and the pseudoscalar (Goldstone) mesons.

The form of the effective Lagrangian is given by the symmetry conditions [3]

$$L = i\bar{q}\gamma^\mu\partial_\mu q - M\bar{q}\exp\{i\gamma_5\tau^a\pi^a/f_\pi\}q \tag{9}$$

where M denotes the constituent quark mass with $M = 350$ MeV and the dimensional constant $f_\pi = 93$ MeV.

Such a Lagrangian has been obtained, for example, in [15] after the spontaneous breaking of the chiral symmetry in the instanton QCD vacuum but actually it has a much wider context (see [16], where it has been argued that one can use the Lagrangian

[2]One looses the longitudinal logarithm due to the fact that the structure functions $f_1(x,Q^2)$, $g_1(x,Q^2)$ correspond to the s-channel discontinuity (imaginary part of the amplitude).

[3]For the sake of simplicity here we consider the $SU(2)$ flavour group but one can easily take into account the s-quark and all the octet of the pseudoscalar mesons putting in (9) the Gell-Mann matrices λ^a instead of the Pauli ones τ^a and continuing the sum over a up to $a = 8$.

(9) up to rather large momenta ~ 1 GeV/c). The same Lagrangian has been successfully used in [11] for the explanation of the "spin crisis" and the Gottfried sum rule violation

$$\int_0^1 \left[F_2^p(x,Q^2) - F_2^n(x,Q^2)\right]\frac{dx}{x} = 0.24 \pm 0.016 < \frac{1}{3}\ ,$$

where $F_2^p(x,Q^2)$ and $F_2^n(x,Q^2)$ are the proton and neutron structure functions measured in DIS.

As it has been discussed in [11] the reasonable upper limit of the validity of Lagrangian (9) is the mass of the η'-meson (958 MeV ~ 1 GeV). This pseudoscalar meson is not included in (9). Due to the axial anomaly it is mixed with the $\tilde{G}_{\mu\nu}G_{\mu\nu}$ gluon operator [4]. Thus for the momenta larger than 1 GeV/c ($m_{\eta'}$) one has to take into account the gluon degrees of freedom explicitly.

So in the next section we shall use perturbative QCD evolution equation (4) in our calculation if the gluon momenta are large enough ($|k_{g,T}|^2 > t_0 = 1$ (GeV/c)^2) and the equation originated from effective Lagrangian (9) for a smaller k_T ($\mu \le |k_T| \le M_{\eta'}c \approx 1$ GeV/c). The main vertex (which gives the leading logarithm and can be obtained from the Lagrangian (9)) is the single pion emission one. In other words we deal with the γ_5-theory with the vertex $M\gamma_5\tau^a/f_\pi$ which has been first considered for the deep inelastic scattering leading logarithm structure function by Gribov and Lipatov [6]. In such a theory one has an evolution equation analogous to the DGLAP one. The equation has been discussed in detail in [11] and here we shall use it within the DL approximation only. With the double-logarithmic accuracy one has

$$\frac{\partial q^i(x,Q^2)}{\partial \ln Q^2} = \frac{M^2}{16\pi^2 f_\pi^2}\Big\{\sum_j \int_x^1 \Phi_{ij}(z) q^j(x/z,Q^2)\frac{dz}{z} - \phi q^i(x,Q^2)\Big\}\ , \tag{10}$$

$$\frac{\partial \Delta q^i(x,Q^2)}{\partial \ln Q^2} = \frac{M^2}{16\pi^2 f_\pi^2}\Big\{\sum_j \int_x^1 \Delta\Phi_{ij}(z) \Delta q^j(x/,Q^2)\frac{dz}{z} - \phi \Delta q^i(x,Q^2)\Big\} \tag{11}$$

where $q^i = q^{i+} + q^{i-}$ (and $\Delta q^i = q^{i+} - q^{i-}$) denotes the sum (and the difference) of the quark densities with the positive (q^+) and negative (q^-) helicities, $f_1(x,Q^2) \sim q(x,Q^2)$ while $g_1(x,Q^2) \sim \Delta q(x,Q^2)$, the indices i and j denote the flavour of the quark and the kernels Φ_{ij} are given by the expressions [6], [11]

$$\begin{aligned} \Phi_{ij}(z) &= 2N_{ij}(1-z)\ , \\ \Delta\Phi_{ij}(z) &= -2N_{ij}(1-z) \end{aligned} \tag{12}$$

where $N_{ij} = 1$ for the charged pion emission and $N_{ij} = 1/2$ for the π^0 emission, i.e. $N_{ij} = 1 - \delta_{ij}/2$. The second term in (10), (11)

$$\phi = \phi_i = \sum_j \int_0^1 \Phi_{ij}(z)dz = \sum_j N_{ij} = 3/2 \tag{13}$$

reflects the conservation low. After the interaction (new parton emission) a parton which carries a momentum fraction x produces a new particle with the momentum fraction xz

[4] This is an important new feature which explains in particular the $U(1)$ problem.

and simultaneously the initial parton (with the fraction x) disappears. Within the DL approximation one may omit this last term proportional to ϕ as it does not give the double-logarithmic contribution. For the same reason we did not write in (10), (11) the contribution coming from the splitting of the pion into the quark-antiquark pair as the corresponding kernel $\Phi_\pi = 2N_{ij}z$ vanishes when $z \to 0$.

Therefore the only contribution which one should take into account within the DL approximation comes from the $z \to 0$ limit of the $\Phi_{ij}(z)$ kernel and we can come back to equation (4) putting the coupling $G(t_m)$ in the form

$$G(t_m) = \frac{C_F}{2\pi}\alpha_s(t_m)[1-\theta(t_0-t)\theta(t_0-t')] + g\theta(t_0-t)\theta(t_0-t') \tag{14}$$

where the constant g depends on the t-channel isospin and the sort of the function under consideration ($f_1(x,Q^2)$ or $g_1(x,Q^2)$). For the case of $f_1(x,Q^2)$ (i.e $q(x,Q^2)$)

$$g^{I=0} = \frac{3M^2}{16\pi^2 f_\pi^2}\ , \quad g^{I=1} = -\frac{M^2}{16\pi^2 f_\pi^2}\ , \tag{15}$$

while for the case of $g_1(x,Q^2)$ (i.e. $\Delta q(x,Q^2)$) the constant g changes the sign in accordance with relations (12)

$$g^{I=0} = -\frac{3M^2}{16\pi^2 f_\pi^2}\ , \quad g^{I=1} = \frac{M^2}{16\pi^2 f_\pi^2}\ . \tag{16}$$

The inhomogeneous term in (4) is now equal to

$$A_0(t,\beta) = \frac{C_F}{2\pi}\alpha_s(t/\beta)\theta(t-t_0) + g\theta(t_0-t)\ . \tag{17}$$

The smallness of the factor $M^2/(16\pi^2 f_\pi^2) \sim 0.1$ justifies here the possibility of using the leading logarithmic evolution equations in the region of rather small k_T starting from the $k_T = M$. Up to the $|k_T^2| = t_0 = 1(\mathrm{GeV/c})^2$ we will use the evolution equation given by the effective Lagrangian (9) (the second term in (14)) and then come back to the conventional perturbative QCD. The form of the θ-function written in the first term of (14) reflects the fact that the transverse momentum of the gluon in Fig. 1 $k_{g,T} = k'_T - k_T$ is close to the largest value of the momentum k_T or k'_T. Thus, within the accuracy of the DL approximation when either $k_T \gg k'_T$ or $k_T \ll k'_T$ we can put $k_{g,T} = max\{k'_T, k_T\}$ and write the $\theta(|k_{gT}^2| - t_0)$ as $1-\theta(t_0-t)\theta(t_0-t')$ [5].

If one puts the factor like $\theta(t-t_0)\theta(t'-t_0)$ instead of the square brackets in (14) he will loose any possibility to go back to the small-k_T region ($|k_T^2| < t_0$) after the first iteration of the perturbative QCD evolution. In this case the non-perturbative (the second term in (14) coming from effective Lagrangian (9)) part of the evolution may change only the "initial" distributions at $t = t_0$ but nothing else. All the asymptotic behaviour (large Q^2 or small x) of the structure functions $f_1(x,Q^2)$ and $g_1(x,Q^2)$ would be the same as it is predicted by the conventional perturbative QCD without any pion emission/exchange. For the coupling constant simple one loop expression $\alpha_s(k^2) = 4\pi/[b\ln(k^2/\Lambda^2)]$ with $\Lambda = 200$ MeV/c has been used.

[5] We remind that $t = |k_T^2|$, $t' = |(k'_T)^2|$.

Strictly speaking we cannot use the equation (4) to calculate the spin-dependent structure function $g_1(x,Q^2)$ at very small x. The equation (4) sums up all the ladder diagrams (Fig. 1) but the function $g_1(x,Q^2)$ corresponds to the negative signature amplitude where the non-ladder contributions coming from an additional gluon exchange are important at small x. In the DL approximation limit the non-ladder graphs give us the terms of the order of $(\alpha_s \ln^2 x)^n$ [9]. Fortunately this non-ladder terms are not too important numerically. In the non-singlet case at large N_c they are suppressed by the factor $1/N_c^2$. From the asymptotical point of view one can estimate the role of the non-ladder contributions comparing the small-x behaviour (eq. (2)) of the functions $f_1(x,Q^2)$ (where there are no any non-ladder leading logarithmic contribution) and $g_1(x,Q^2)$. For the negative signature amplitude ($g_1(x,Q^2)$) the asymptotic power of x is 4% larger (see (3)). To take this fact into account, at least approximately, we increase by 8% the "effective" value of α_s in our computations of the non-singlet components of $g_1(x,Q^2)$ as the value of $\omega^{(-)}$ is proportional to $\sqrt{\alpha_s}$ what follows from (3). Due to the zero spin of the pion there are no any non-ladder double-logarithmic contributions originated from the pion exchange. So no any additional modification of the second term of the coupling $G(t_m)$ in (14) is needed.

2.2 Singlet $g_1(x,Q^2)$.

The linear equation which sums up all the ladder double logarithms in the singlet case has exactly the same form (4) as before. The only difference is that now the equation has the matrix form. Indeed, in the singlet channel there appear the graphs with the two gluons (instead of two quarks) in the t-channel (Fig. 2). These quark and gluon t-channel states mix with each other and one has to consider the system of two equations which describes the evolution of quarks and gluons simultaneously. From the formal point of view this means that the amplitudes, $A(t,\beta)$ and the kernels, G should be written as the matrices A^c_d and G^c_d where the upper index denotes the sort of the current parton ($c=q$ for a quark and $c=g$ for a gluon) while the lower one denotes the type of a parent parton for G^c_d or of a target one for the amplitude A^c_d. The equation for the matrix elements reads

$$A^c_d(t,\beta) = (A_0)^c_d(t,\beta) + \sum_{r=q,g} \int_\beta^1 \frac{d\beta'}{\beta'} \int_{\mu^2}^{t_m} \frac{dt'}{t'} \hat{G}^c_r A^r_d(t',\beta')\ . \tag{18}$$

Let us note that now we discuss the polarized distribution $g_1(x,Q^2)$ only. For the unpolarized structure function $f_1(x,Q^2)$ the low-x asymptotics is governed by the pure gluon amplitude as the gluon-gluon splitting kernel $P^G_G(z)$ has the $1/z$ singularity at $z\to 0$. In the complex momentum (j) plane it corresponds to the singularity at $j=1$ and leads to the DL asymptotic behaviour $f_{1,S}(x,Q^2)\sim x^{-1}\Phi(\alpha_s \ln(1/x)\ln Q^2)$ with the function Φ not having a powerlike ($\sim x^{-\lambda},\ \lambda>0$) singularity at $x\to 0$. The asymptotics originated from the quark exchange is suppressed by one power of x ($\sim x^0\tilde{\Phi}(\alpha_s \ln(1/x)\ln Q^2)$) and may be neglected in comparison with the gluon contribution. However, for the case of the spin-dependent functions $g_1(x,Q^2)$ the splitting kernels $\Delta P^c_d(z)$ tend to a constant limit at $z\to 0$. The position of their rightmost singularities is $j=0$ [7], [17]. Therefore all the splitting kernels ($q\to gq,\ q\to qg,\ g\to gg,\ g\to q\bar{q}$) give the same double logarithms and should be taken into account.

The matrix G_d^c for the polarized distributions $g_1(x,Q^2)$ has the form [5]

$$\hat{G}_b^a = \frac{\hat{H}_b^a}{2\pi}[1-\theta(t_0-t)\theta(t_0-t')] + \hat{g}_b^a\theta(t_0-t)\theta(t_0-t') \tag{19}$$

where the matrix $\hat{H}$ looks like [7], [5]

$$\hat{H} = \begin{pmatrix} 4N_c\alpha_s(\tilde{t}) & 2C_F\alpha_s(t) \\ -n_f\alpha_s(t') & C_F\alpha_s(t_m) \end{pmatrix} . \tag{20}$$

Here n_f is a number of active quark flavours and $\tilde{t} = t'\beta/\beta'$. The important question which arguments have the running coupling constants α_s in (20) will be discussed in the next subsection. If some argument of running coupling ($\tilde{t}$, t, t' or t_m) becomes smaller that t_0 we put it equal to t_0. The matrix $\hat{g}$ is

$$\hat{g} = \begin{pmatrix} 0 & 0 \\ 0 & g \end{pmatrix} . \tag{21}$$

Of course the last term describing the non-perturbative pion emission does only presence in the quark-quark splitting with the constant $g = -3M^2/(16\pi^2 f_\pi^2)$ which corresponds to the zero isospin (see (15), (16)). The Born term in (18) reads

$$A_0(t,\beta) = \frac{\hat{H}_0}{2\pi}\theta(t-t_0) + \hat{g}\theta(t_0-t) . \tag{22}$$

with $\hat{H}_0$ given by the relation

$$\hat{H}_0 = \begin{pmatrix} 4N_c\alpha_s(t_0) & 2C_F\alpha_s(t) \\ -n_f\alpha_s(t_0) & C_F\alpha_s(t/\beta) \end{pmatrix} . \tag{23}$$

As in the non-singlet case the contribution of the non-ladder gluons (which also give the double logarithms for the negative signature amplitude at small x [9]) will be taken effectively into account by the numerical correction of the matrix $\hat{H}$. Instead of $\hat{H}$ we will use in our computations the matrix $\hat{H}_{eff} = \hat{H} + \hat{\delta}$ with

$$\hat{\delta} = \begin{pmatrix} -2.016\alpha_s(\tilde{t}) & -0.179\alpha_s(t) \\ 0.168\alpha_s(t') & 0.025\alpha_s(t_m) \end{pmatrix} . \tag{24}$$

The elements of the $\hat{\delta}$-matrix reflects the nonladder contribution at the complex momentum $j = j_r$ close to the rightmost singularity of the DL approximation perturbative QCD function $g_1(x,Q^2)$, i.e. at $z = j\sqrt{2\pi/[N_c\alpha_s]} = 3.45$ (for $n_f = 4$) [5]. Therefore it provides the correct asymptotic behaviour of our solution at $x \to 0$. It has been checked that such an approximation reproduce the pure QCD DL approximation results [5] with the 15% accuracy within the interval of $x = 10^{-1} - 10^{-5}$ and $Q^2 = 10 - 2000$ (GeV/c)^2.

Finally, to obtain the singlet component of the structure function $g_1(x,Q^2)$ one has to put the quark component of the amplitude A_d^q into (5)

$$g_{1,S}^d(x,Q^2) = e_d^2\delta(1-x) + \frac{\sum_{q=1}^{n_f} e_q^2}{n_f}\int_{\mu^2}^{S_m} A_d^q(t,\tilde{\beta})\frac{dt}{t} \tag{25}$$

with $\tilde{\beta} = x + t/s$. The equations (18-25) with the $n_f = 4$ will be used in section 3 in order to estimate the small-x behaviour of the singlet component of the structure function $g_1(x, Q^2)$ in the presence of the non-perturbative, pion induced interactions at rather low k_T^2 ($\sim 0.1 - 1$ (GeV/c)^2) given by effective Lagrangian (9).

2.3 Argument of the running coupling

Let us discuss now which argument of α_s we are to use in the master equation (18). The simplest way to answer this question was proposed in [18]. One is to calculate the logarithmic contribution to the running coupling α_s coming from a new sort of a light quark and then to use the fact that owing to the renormalization group all the other contributions to α_s are to have the same q^2-dependence as the quark loop has. In the case of the quark-quark splitting kernel (or the non-singlet function) the only possibility to include the new quark loop is to insert it into the s-channel gluon propagator, where one obtains the logarithmic (dm^2/m^2) integration over the quark-antiquark pair mass m (i.e. over the virtual gluon mass). The logarithmical behaviour continues up to the $m^2 \sim t_m = t\beta'/\beta$. At larger $m^2 > t_m$ the longitudinal component of the t-channel quark momentum $k_{||}^2 \sim m^2\beta/\beta' \geq t = |k_T^2|$ becomes essentially larger than the transversal one. This destroys both the logarithm (dt/t) in integration over $k_T^2 = t$ and the logarithm in the integral over m^2.

However the prescription $\alpha_s = \alpha_s(t_m)$ is not the universal one. For the quark to gluon (and gluon to quark) splitting kernels we again have to insert an additional quark loop into the gluon (but now the t-channel gluon) propagators. Certainly, here the logarithm depends on the gluon virtuality (t for the P_q^G and t' for the P_G^q kernels).

The situation with the gluon-gluon kernel is more complicated. Now the new quark loop is to be inserted in each gluon propagators (s-channel and t-channel) and into the triple gluon vertex. The t-channel propagators give us the $\ln t$ and $\ln t'$, while the s-channel propagator gives $\ln t_m$ (as in the non-singlet, i.e. P_q^q case). Finally it is easy to see by straightforward calculations that the logarithm coming from the vertex diagram depends on the largest virtuality, i.e. on the t_m. This point has been discussed in more detail in [19] where it has been shown that the vertex and the s-channel gluon logarithmic contributions cancel each other. However, in the case under discussion we have two vertexes. So, the sum of all the logarithms looks like

$$\ln t + \ln t' + \ln t_m - 2\ln t_m = \ln(t'\beta/\beta') \; .$$

In other words the probability of gluon-gluon splitting is proportional to $\alpha_s(\tilde{t})$ with $\tilde{t} = t'\beta/\beta' \leq t'$. To take these running couplings into account one is to use in the master equation (18) the matrix $\hat{H}$ defined in (20) instead of the quantity $\alpha_s(t_m)C_F$ for the non-singlet case.

3 Discussion of numerical results

The results of the computation are presented in Figs. 3-10. For the calculation of the non-singlet structure functions we have used the DL equations (4), (5), (7), (14), (15), (16) with the lower (infrared) limit $\mu = M = 350$ MeV/c, $t_0 = 1$ (GeV/c)^2, $\Lambda = 200$ MeV/c, $n_f = 4$ and the simplest initial condition - the one quark with $\beta = x = 1$ at $t = M^2$ (see (5)); i.e. we have considered deep inelastic scattering on a "free" quark target. [6] We have found the analytical solution of the double-logarithmic integral equation for the non-singlet case which is presented in Appendix. An application of the analytical solution permits us to calculate the non-singlet structure functions for very small x (up to $x = 10^{-7}$). For the singlet case we have solved the DL integral equation by the iteration method with a typical number of iterations $15 \div 17$ and a number of points for integration over β' (t') in (18) is equal to 142 (380). The accuracy of the performed calculations of the singlet structure functions is higher than 5%.

In Fig. 3a (4a) the x-dependence of the isovector structure function $f^{I=1}_{1,NS}(x,Q^2)$ ($g^{I=1}_{1,NS}(x,Q^2)$) is shown at $Q^2 = 10$, 30, 100 and 300 (GeV/c)^2. For $f^{I=1}_{1,NS}(x,Q^2)$ the power of the asymptotic behaviour ($x^{-\lambda}$) reveals itself at $x < 10^{-3}$ and for $g^{I=1}_{1,NS}(x,Q^2)$ this happens even at $x < 10^{-2}$. It follows from the analytical solution that the asymptotical behaviour of the non-singlet structure function at small x and $Q^2 > t_0 = 1$ (GeV/c)^2 looks like (see equation (49) in Appendix)

$$f_{NS}(x,Q^2) = F_1 x^{-\lambda_1}\{\ln^{\kappa_1}(Q^2/\Lambda^2) - \ln^{\kappa_1}(\mu^2/\Lambda^2) + \kappa_1 \ln^{\kappa_1 - 1}(Q^2/\Lambda^2)[\psi(1) - \psi(\lambda_1)]\} \quad (26)$$

where F_1 denotes some constant and $\psi(\zeta)$ is the digamma function [20]. In (26) λ_1 is the solution of equation (46) (see Appendix) with the largest value and $\kappa_1 = 8/[(33-2n_f)\lambda_1]$. The x-dependence of the effective power $\lambda = -\partial \ln f_1(x,Q^2)/\partial \ln x$ (or $-\partial \ln g_1(x,Q^2)/\partial \ln x$ for g_1) is shown in Fig. 3b (4b). Due to the positive sign of the constant g for the case of the isovector function $g^{I=1}_{1,NS}(x,Q^2)$ here (Fig. 4b) the value of λ at small x ($\lambda = 0.30$) is larger than in Fig. 3b ($\lambda = 0.24$), i.e. for $f^{I=1}_{1,NS}(x,Q^2)$ where g is negative (see (15), (16)).

To demonstrate better the role of the non-perturbative (pion emission) contribution, in Fig. 3c (4c) we plot the ratio R of the whole function $f^{I=1}_{1,NS}(x,Q^2)$ ($g^{I=1}_{1,NS}(x,Q^2)$) to the pure perturbative QCD prediction given by the solution of the same equations (4), (5), (7), (14) with the same initial condition, but with $g = 0$. In the case of $f^{I=1}_{1,NS}(x,Q^2)$ this ratio at small x tends to the constant limit close to $R \approx 0.5$. As here the value of g is negative the system trys to go out of the region $|k_T^2| < t_0$. Thus the behaviour of the function $f^{I=1}_{1,NS}(x,Q^2)$ is close to the pure perturbative QCD case and only the normalization of the asymptotics becomes smaller (about 2 times). On the contrary, the analogous ratio R for the polarized function $g^{I=1}_{1,NS}(x,Q^2)$, where $g > 0$ [7], increases with the energy (i.e. $1/x$), the effective power λ here is larger (0.30) than in the pure perturbative QCD case. In particular, in the HERA kinematical range (say, at $x = 10^{-3} - 10^{-4}$, $Q^2 = 10 - 300$ (GeV/c)^2) this ratio reachs the values of about 2.5-2.9 It is a large effect which may be very useful for the explanation of a large difference between the proton and neutron structure functions $g_1^p(x,Q^2) - g_1^n(x,Q^2)$ in the region of $x \sim 10^{-2}$ [13].

[6] As it has been discussed at the end of Sect. 2.1 in [4] for the $g_{1,NS}(x,Q^2)$ the QCD coupling α_s has been multiplied by 1.08 to take into account effectively contributions of non-ladder Feynman graphs.

[7] Here we have two minuses: one due to the spin-flip nature of the γ_5 quark-pion vertex and another one due to the isovector nature of the pion (i.e. the matrix τ^a in the vertex). Finally one has $g > 0$ for the isovector component of $g^{I=1}_{1,NS}(x,Q^2)$

The results of our calculations for the t-channel isospin equal to zero are presented in Figs. 5 and 6. The value of λ for the structure function $f_{1,NS}^{I=0}(x,Q^2)$ changes dramatically due to the pion contribution and becames equal to ≈ 0.5 as one can see from Fig. 5b. It is remarkable that we get the value of λ which agrees very well with the prediction of the Regge phenomenology. We would like to stress that we have not free parameters in our approach. The only parameter which is not absolutely reliably fixed from experimental data is the mass of the constituent u and d quarks which has been put equal to 350 MeV. We can see from Fig. 5a that the behavior $\sim x^{-\lambda}$ is valid from rather large $x \sim 0.01$. We can see also from Fig. 5c that the ratio of all the contributions to $f_{1,NS}^{I=0}(x,Q^2)$ including the non-perturbative ones to the pure perturbative QCD contributions is larger than 40 at $x < 10^{-4}$. Hence the small-x behaviour of the non-singlet structure function $f_{1,NS}^{I=0}(x,Q^2)$ is changed crucially by the non-perturbative effects. For the spin-dependent structure function $g_{1,NS}^{I=0}(x,Q^2)$ the pion exchange contributions are not so important as for $f_{1,NS}^{I=0}(x,Q^2)$. Indeed, as we can see from Fig. 6b the value of λ (0.25) does not differ crucially from its value predicted in the framework of the perturbative QCD ($\lambda = 0.22$ [21]). This is due to the negative value of the constant g given by (16). We would like to remark that the power λ for $g_{1,NS}^{I=0}(x,Q^2)$ for the isotopical singlet channel is smaller than that one for the $I=1$ channel ($\lambda = 0.30$) for which the value of the pion exchange constant g is positive in accordance with (16). Vice versa for the unpolarized structure function $f_{1,NS}(x,Q^2)$ the power λ for the isosinglet channel is larger than that one for the isotriplet channel as for the former case g is large and positive and for the latter one the pion exchange constant g is negative. We would like to remark that the values of the effective powers λ at $x \leq 10^{-3}$ do not practically depend on Q^2 as we can see from Figs. 3-6. Such a behaviour is in accordance with the prediction of formula (26). At low x the effective powers λ are very close to their asymptotical values (λ_1) which can be found as solutions of equation (46) (see Appendix).

For the singlet component of the spin-dependent function $g_1(x,Q^2)$ calculated in a pure "ladder" approximation (with $\hat{\delta} = 0$) the set of the curves is shown in Figs. 7, 8 where the evolution starts from the initial target gluon and quark, respectively. In both cases at low x the behaviour of $g_1(x,Q^2) \sim x^{-\lambda}(Q^2)^{\gamma}$ have the powerlike character with an almost constant values of $\lambda \approx 1.48$ and $\gamma \approx 0.5$. When the evolution starts from the gluon target the role of the pion induced interactions is negligible and the ratio R_G (of the whole singlet function $g_1(x,Q^2)$ to the pure perturbative QCD prediction) is close to 1 (see Fig. 7c), while for the initial quark target the value of R_q decreases with increasing of $1/x$ and reaches $R_q \approx 0.7$ at $x \leq 0.01$ (see Fig. 8c). All these features reflect the fact that due to a larger spin and colour charge of the gluons they play the dominant role in the singlet structure function $g_1(x,Q^2)$ evolution especially at small x. As the gluons do not interact with the pions the ratio $R_G \approx 1$. In the latter case the initial quark emits the pions at the beginning of the evolution. Therefore the ratio R_q falls down. Then (somewhere in the region of $x \sim 0.1 - 0.01$), after the P_q^G splitting kernel the evolution switches into the gluon channel. Hence it becomes mainly of the gluon nature and the value of R_q is frozen up (does not change any more at x smaller than 0.01).

As it has been explained above to estimate [8] the contribution of non-ladder graphs

[8] One may say to simulate.

we replace the matrix $\hat{H}$ in (19) and (18) with $\hat{H}_{eff} = \hat{H} + \hat{\delta}$ where $\hat{H}$ and $\hat{\delta}$ have been defined in (20), (24). The results of our calculations are presented in Fig. 9 and Fig. 10. We see from Fig. 9a, 10a that the contributions of non-ladder graphs do not change the power-like asymptotical behaviour of $g_{1,S}$ both for the initial gluon and quark. For $x < 10^{-2}$ the effective powers λ for initial gluon and quark cases are approximately equal to each other. However as in a pure perturbative QCD case [5] for the singlet structure functions the non-ladder contribution diminishes the power λ. For small x the value of $\lambda \approx 1.33$ in Figs. 9, 10 is smaller than in Fig. 7b, Fig. 8b ($\lambda \approx 1.48$) and as in the non-singlet case λ is almost independent on Q^2 for $x < 10^{-2}$. The relative contribution of the non-ladder graphs to $g_{1,S}(x, Q^2)$ increases with a decrease of x as we can see from Figs. 9c, 10c. Indeed, the ratio R^{NL} of a sum of the ladder and non-ladder graph contributions to the ladder graph ones is approximately equal to 0.8 at $x = 0.1$ and becomes equal to ≈ 0.3 at $x = 10^{-4}$ both for the initial gluon (R_G^{NL}) and quark (R_q^{NL}) the pion exchange contributions being taken into account in all calculations.

4 Conclusion

The double-logarithmic integral equation describing both the perturbative QCD and non-perturbative (pion exchange) contributions to the structure functions at small Bjorken x has been proposed. The analytical solution of the equation for the non-singlet structure functions ($f_{1,NS}(x, Q^2)$ and $g_{1,NS}(x, Q^2)$) has been found. The powerlike asymptotical behaviour ($\sim x^{-\lambda_1}$) of the structure functions at low x has been predicted (see formula (26)). The effect of the non-perturbative pion induced interaction on the small x asymptotical behaviour of the double-logarithmic structure functions for $Q^2 > 1$ (GeV/c)^2 depends strongly on the sign of the pion coupling constant g as one can see from Figs. 3-6. The pion exchange increases significantly the normalization factor of $f_{1,NS}^{I=0}(x, Q^2)$ and $g_{1,NS}^{I=1}(x, Q^2)$ for positive values of g and decreases it appreciably for $f_{1,NS}^{I=1}(x, Q^2)$ and $g_{1,NS}^{I=0}(x, Q^2)$ as $g < 0$. For the t-channel with the isospin $I = 1$ the effect of the pion exchange leads both to a decrease of the difference of the proton and neutron structure functions $F_2^p(x, Q^2) - F_2^n(x, Q^2)$ at small x and to an increase of $g_1^p(x, Q^2) - g_1^n(x, Q^2)$. The former effect gives a contribution which leads to the Gottfried sum rule violation observed by NMC [12]. The latter one is presumably related with the large difference of $g_1^p(x, Q^2) - g_1^n(x, Q^2)$ measured in [13]. Due to the large and positive value of the pion exchange constant ($g = 0.27$ in accordance with (15)) the non-perturbative contributions to the small-x asymptotical behaviour of $f_{1,NS}^{I=0}(x, Q^2)$ become very important.

The logarithmic derivatives of the structure functions over $\ln(1/x)$ are more stable and do not differ significantly from the pure perturbative QCD predictions except the case of $f_{1,NS}^{I=0}(x, Q^2)$ when λ changes crucially due to the pion exchange. It is remarkable that for this case the logarithmic derivative, λ at small x becomes equal to ≈ 0.5 which is in agreement with its phenomenological Regge pole value.

Our calculation of the flavour singlet structure functions demonstrates a powerlike dependence both on x and Q^2 ($g_{1,S} \sim (Q^2)^{\gamma} x^{-\lambda_1}$). The role of the "soft" ($k_T < 1$ GeV/c) region is not so important for the singlet case, as here the t-channel gluons (which do not emit the pions) govern the small-x evolution. It is demonstrated that the pion exchange decreases $g_{1,S}$ for the initial quark and does not practically change the structure function for the parent gluon. Our estimates of the role of the non-ladder Feynman graph contributions show that they decrease values of $g_{1,S}$ and their relative contributions increase with a decrease of x. In spite of the fact that the singlet component of $g_1(x, Q^2)$ is much more infrared stable, unfortunately, one cannot consider the results presented in Figs. 7-10 as true theoretical predictions. The values of the logarithmic derivative $\lambda \approx 1.48$ (without the non-ladder graph contributions) and $\lambda \approx 1.33$ (a sum of the ladder and non-ladder graph contributions) are too large and the next-to-leading order corrections are probably crucially important. Strictly speaking the original double-logarithmic approximation is valid for $\gamma \ll 1$ and $\lambda \ll 1$ only. Nevertheless, we hope that our results reproduce correctly the main qualitative features of the small-x parton distributions ($f_{1,NS}(x, Q^2)$ and $g_1(x, Q^2)$) and give a true estimate of the role playing by the "soft" ($k_T < 1$ GeV/c) region at small x .

5 Appendix

Here the analytical solution of equation (4) for the non-singlet case is considered. It is convenient to introduce new variables

$$\begin{aligned} y &= \ln(t/\Lambda^2), \quad z = -\ln(\beta), \quad y_0 = \ln(t_0/\Lambda^2), \\ y' &= \ln(t'/\Lambda^2), \quad z' = -\ln(\beta'), \quad u = \ln(\mu^2/\Lambda^2) \end{aligned} \tag{27}$$

then equation (4) for $y < y_0$ looks like

$$\begin{aligned} A(y, z) = g + g \int_0^z dz' \int_u^{y_0} \theta(y + z - y' - z') A(y', z') dy' + \\ + \int_0^z \frac{\nu}{y + z - z'} dz' \int_{y_0}^{y+z-z'} \theta(y + z - y_0 - z') A(y', z') dy' \end{aligned} \tag{28}$$

where $\nu = 2C_F/b = 8/(33 - 2n_f)$ and g has been defined by (15), (16). It is easy to see from (28) that

$$\frac{\partial A(y, z)}{\partial z} - \frac{\partial A(y, z)}{\partial y} = g \int_u^y A(y', z) dy' \ . \tag{29}$$

Differentiation of relation (29) over y gives the differential equation valid at $y < y_0$

$$\frac{\partial^2 A(y, z)}{\partial y \partial z} - \frac{\partial^2 A(y, z)}{\partial y^2} = g A(y, z) \ . \tag{30}$$

Putting in (29) $y = u$ we get the following boundary condition:

$$\left[\frac{\partial A(y, z)}{\partial z} - \frac{\partial A(y, z)}{\partial y}\right]\Big|_{y=u} = 0 \ . \tag{31}$$

For $z = 0$ we have from (28) that

$$A(y, 0) = g \ . \tag{32}$$

Let us define the function ω

$$\omega(y,\rho) = \int_0^{\infty} \exp\{-\rho z\} A(y,z) dz \tag{33}$$

which for $y < y_0$ ($y > y_0$) will be denoted as ω_1 (ω_2). It follows immediately from (30), (31) and (32) that ω_1 looks like

$$\omega_1(y,\rho) = C_1(\rho)\exp\{(y-u)(\rho/2+R)\} + \\ +(\rho/2-R)[1-C_1(\rho)/(\rho/2+R)]\exp\{(y-u)(\rho/2-R)\} \tag{34}$$

where $R = \sqrt{\rho^2/4 - g}$ and $C_1(\rho)$ is an arbitrary function which will be found below.

For $y > y_0$ we get from (4), (7), (14) the integral equation

$$A(y,z) = \frac{\nu}{y+z} + \int_0^z \frac{\nu}{y+z-z'} dz' \int_u^{y+z-z'} A(y',z') dy' \; . \tag{35}$$

The solution of (35) obeys the differential equation [10], [21]

$$\frac{\partial}{\partial y}\Big\{ y\Big(\frac{\partial}{\partial z} - \frac{\partial}{\partial y}\Big) A(y,z) \Big\} = \nu A(y,z) \tag{36}$$

with the boundary condition at $y = y_0 + \epsilon$, $\epsilon \to 0$

$$\Big[\frac{\partial A(y+\epsilon,z)}{\partial z} - \frac{\partial A(y+\epsilon,z)}{\partial y}\Big]\Big|_{y=y_0} = \frac{\nu}{y_0}\int_u^{y_0} A(y',z) dy' \; . \tag{37}$$

To solve equation (36) we apply the Laplace transformation (33) remembering that for $z = 0$ and $y > y_0$

$$A(y,0) = \frac{\nu}{y} \tag{38}$$

which can be easily got from (35). It follows from (36) that ω_2 looks like [10], [21]

$$\omega_2(y,\rho) = C_2(\rho)(\rho y)^{-1/2}\exp\{\rho y/2\} W_{\kappa-1/2,\,0}(\rho y) \tag{39}$$

where $W_{k,m}(\zeta)$ denotes the Whittaker function defined as in [20], $\kappa = \nu/\rho$ and $C_2(\rho)$ is an arbitrary function of ρ but not y. Applying the Laplace transformation to (37) and remembering (33), (38) we get the formula

$$\rho\omega_2(y_0,\rho) - \frac{\partial \omega_2(y,\rho)}{\partial y}\Big|_{y=y_0} = \frac{\nu}{y_0}\Big[1 + \int_u^{y_0} dy'\omega_1(y',\rho)\Big] \tag{40}$$

which relates $C_1(\rho)$ and $C_2(\rho)$ due to (34) and (39). Putting $y = y_0 - \epsilon$ in (28) and $y = y_0 + \epsilon$ in (35) and making use of the Laplace transformation to the difference between these two equations we have for $\epsilon \to 0$ another boundary condition

$$\omega_2(y_0,\rho) - \omega_1(y_0,\rho) = \Big[\nu\frac{e^{\zeta/2}}{\sqrt{\zeta}} W_{-1/2,\,0}(\zeta) - g/\rho\Big]\Big[1 + \int_u^{y_0} dy\,\omega_1(y,\rho)\Big] \tag{41}$$

where $\zeta = \rho y_0$. Formula (41) gives the second relation for $C_1(\rho)$ and $C_2(\rho)$. Then we can easily found $C_1(\rho)$ and $C_2(\rho)$ from (40) and (41) remembering (34) and (39) which are

$$C_1(\rho) = \frac{(\rho/2 + R)}{2\sinh(\eta)}[W_{\kappa,\,1/2}(\zeta)/D(\rho) - \exp\{-\eta\}]\,, \tag{42}$$

$$C_2(\rho) = \frac{\nu \exp\{-\rho u/2\}}{D(\rho)}\,, \tag{43}$$

where

$$D(\rho) = \Big\{\Big[\frac{\nu e^{\zeta/2}}{\sqrt{\zeta}} W_{-1/2,\,0}(\zeta) - \frac{g}{\rho} + \frac{\rho}{2}\Big] W_{\kappa,\,1/2}(\zeta) - \frac{\nu W_{\kappa-1/2,\,0}(\zeta)}{\sqrt{\zeta}}\Big\}\frac{\sinh(\eta)}{R} + \cosh(\eta) W_{\kappa,\,1/2}(\zeta) \tag{44}$$

with $\eta = (y_0 - u)R$, $\kappa = \nu/\rho$.

The general solution of equation (4) for the non-singlet case is given by the inverse Laplace transformation

$$A(y,z) = \frac{1}{2\pi i}\int_{a-i\infty}^{a+i\infty} d\rho \exp\{\rho z\}\omega(y,\rho) \tag{45}$$

with the parameter a in (45) chosen so that the integration contour runs to the right from all singularities of $\omega(y,\rho)$ in the complex ρ-plane. The function $\omega(y,\rho)$ at $y < y_0$ has been defined by (34), (42), (44) and at $y > y_0$ it can be found from (39), (43), (44). Taking into account analytical properties of the Whittaker functions $W_{\kappa-1/2,\,0}(\eta)$ and $W_{\kappa,\,1/2}(\zeta)$ we can easily prove with the help of (44) that $D(\rho)$ is an analytical function of ρ in the complex ρ-plane with a cut from $-\infty$ up to 0. It can have zeros at real ρ which we denote as λ_n ($\lambda_1 > \lambda_2 > \lambda_3 > \ldots$). The solutions of the equation

$$D(\rho) = 0 \tag{46}$$

are the poles of $C_1(\rho)$, $C_2(\rho)$ what follows from (42), (43) and hence they are also the poles of $\omega_1(y,\rho)$, $\omega_2(y,\rho)$ as we can see from (34) and (39). Let us denote the derivative of $D(\rho)$ over ρ at $\rho = \lambda_n$ as D_n than the pole contribution to integral (45) for large y ($y > y_0$) is equal to

$$A_n(y,z) = \frac{\nu}{D_n\sqrt{\lambda_n y}} \exp\{\lambda_n(z + y/2 - u/2)\} W_{\kappa_n - 1/2,\,0}(\lambda_n y) \tag{47}$$

where $\kappa_n = \nu/\lambda_n$. For $y > y_0$ the asymptotical behaviour of $A(y,z)$ at large z (small β) is determined by the rightmost singularity of $\omega_2(y,\rho)$ and looks like

$$A(t,\beta) \sim A_1(t,\beta) = S_1 \beta^{-\lambda_1}(t/\Lambda^2)^{\lambda_1/2}[\lambda_1 \ln(t/\Lambda^2)]^{-1/2} W_{\kappa_1 - 1/2,\,0}(\lambda_1 \ln(t/\Lambda^2)) \tag{48}$$

where S_1 denotes a constant equal to $\nu \exp\{-\lambda_1 u/2\}/D_1$. We have used in (48) relations (27). The dependence of $A_1(t,\beta)$ on t and β given by (48) has the same form as for the perturbative QCD which is described by formulae (60) and (39) in [21]. It has been shown in [21] that substituting (48) in (5) we can get for the small-x asymptotics of the non-singlet structure function the final relation

$$f_{NS}(x,Q^2) = \lambda_1^{\kappa_1}\exp\{-\lambda_1 u/2\}D_1^{-1}x^{-\lambda_1}\{\ln^{\kappa_1}(Q^2/\Lambda^2) - \ln^{\kappa_1}(\mu^2/\Lambda^2) + \kappa_1\ln^{\kappa_1-1}(Q^2/\Lambda^2)[\psi(1)-\psi(\lambda_1)]\} \quad (49)$$

which coincides with (26) if we take into consideration that $F_1 = \lambda_1^{\kappa_1}\exp\{-\lambda_1 u/2\}/D_1$.

As it has been explained in the text we simulate the non-ladder Feynman graph contributions to the non-singlet structure function $g_{1,NS}(x,Q^2)$ replacing ν by $\gamma = 1.08\nu$ in $G(t_m)$ in equation (4) but not changing the inhomogeneous term A_0. In the same way as we have got formulae for $\omega_1(y,\rho)$ and $\omega_2(y,\rho)$ we can obtain now that for $y > y_0$

$$\omega_2(y,\rho) = \Big\{\frac{-\tau\exp\{-\zeta/2\}}{W_{\sigma,\,1/2}(\zeta)} + \frac{\gamma}{D(\rho)}\Big[\exp\{-u\rho/2\} + \tau\exp\{-\zeta/2\}\frac{\sinh(\eta)}{R}\frac{S}{W_{\sigma,\,1/2}(\zeta)}\Big]\Big\}\frac{\exp\{\rho y/2\}}{\sqrt{\rho y}}W_{\sigma-1/2,\,0}(\rho y) \quad (50)$$

where $\tau = 0.08\nu$, $\sigma = \gamma/\rho$ and

$$S = [\exp\{\zeta/2\}W_{-1/2,\,0}(\zeta)W_{\sigma,\,1/2}(\zeta) - W_{\sigma-1/2,\,0}(\zeta)]/\sqrt{\zeta}\;. \quad (51)$$

Poles of $\omega(y,\rho)$ in the ρ-plane are zeros of the function $D(\rho)$ as before but now it looks like

$$D(\rho) = \gamma S\frac{\sinh(\eta)}{R} + W_{\sigma,\,1/2}(\zeta)\Big[\cosh(\eta) + (\frac{\rho}{2} - \frac{g}{\rho})\frac{\sinh(\eta)}{R}\Big]\;. \quad (52)$$

Introducing a quantity of Z

$$Z = S[\gamma\cosh(\eta) - \tau\exp\{-(y_0-u)\rho/2\}] + W_{\sigma,\,1/2}(\zeta)[R\sinh(\eta) + (\frac{\rho}{2} - \frac{g}{\rho})\cosh(\eta)] \quad (53)$$

we have the formula for $\omega(y,\rho)$ at $y < y_0$

$$\omega_1(y,\rho) = \exp\{(y-u)\rho/2\}\Big\{\frac{\rho}{2}\cosh(w) + R\sinh(w) - \frac{Z}{D(\rho)}\Big[\frac{\rho}{2R}\sinh(w) + \cosh(w)\Big]\Big\} \quad (54)$$

where $w = (y-u)R$. It is easy to see from formulae (50), (54) that though $\omega_1(y,\rho)$ and $\omega_2(y,\rho)$ depend on $R = \sqrt{\rho^2/4 - g}$ but there are no any brunching points at $\rho = \pm 2\sqrt{g}$ as they contain even powers of R only. It can be proven that $\omega_1(y,\rho)$ and $\omega_2(y,\rho)$ have cuts in the complex ρ-plane from $-\infty$ up to 0 and poles for the positive values of ρ which obey equation (46) with $D(\rho)$ given by (52). We would like to remark that there are no poles of $\omega_2(y,\rho)$ which correspond to zeros of the function $W_{\sigma,\,1/2}(\zeta)$. Indeed, the pole contributions of the two terms containing $W_{\sigma,\,1/2}(\zeta)$ in denominator in (50) cancel each other. Formula (26) remains valid for $Q^2 > t_0$ as the non-ladder graph contributions do not change the y-dependence of $\omega_2(y,\rho)$ given by (39) but change $C_2(\rho)$ only which leads to an alteration of the constant F_1 and to the replacement $\kappa_1 = \gamma/\lambda_1$ in (26).

References

[1] V. G. Gorshkov,V. N. Gribov, L. N. Lipatov and G. V. Frolov: *Sov. Journ. Nucl. Phys.* **6** (1967) 95.

[2] V.G.Gorshkov: *Sov. Phys. Uspekhi* **16** (1973) 322.

[3] B. I. Ermolaev, S. I. Manayenkov, M. G. Ryskin: *Z. Phys.* **C69** (1996) 259.

[4] J. Bartels, B. I. Ermolaev, M. G. Ryskin: *Z. Phys.* **C70** (1996) 273.

[5] J. Bartels, B. I. Ermolaev, M. G. Ryskin: *Z. Phys.* **C72** (1996) 627.

[6] V. N. Gribov and L. N. Lipatov: *Sov. Journ. Nucl. Phys.* **15** (1972) 438 and 675.

[7] G. Altarelli and G. Parisi: *Nucl. Phys.* **B126** (1977) 298.

[8] Yu. L. Dokshitser: *Sov. Phys. JETP* **46** (1977) 641.

[9] R. Kirschner and L. N. Lipatov: *Nucl. Phys.* **B213** (1983) 122.

[10] S. I. Manayenkov: *Yad. Fiz.* **60** (1997) 915; *Phys. of Atomic Nuclei.* **60** (1997) 819.

[11] A. A. Anselm and M. G. Ryskin: *Z. Phys.* **C68** (1995) 297.

[12] P. Amaudruz et al.: *Phys. Rev. Let.* **66** (1991) 2712.

[13] D. Adams et al.: *Phys. Lett.* **B329** (1994) 399; **B357** (1995) 248.

[14] V. V. Sudakov: *ZhETP* **30** (1956) 87

[15] D. I. Dyakonov and V. Yu. Petrov: *Nucl. Phys.* **B272** (1986) 457.

[16] A. Manohar, H. Georgi: *Nucl. Phys.* **B234** (1984) 189.

[17] M. A. Ahmed and G. G. Ross: *Nucl. Phys.* **B111** (1976) 441.

[18] S. Brodsky et al.: *Phys. Rev.* **D28** (1983) 228.

[19] E. Levin et al.: *Sov. Journ. Nucl. Phys.* **54** (1991) 867.

[20] E. T. Whittaker, G. N. Watson. A Course of Modern Analysis, Cambridge, 1927.

[21] S. I. Manayenkov: *Z. Phys.* **C75** (1997) 685.

Figure captions

Fig. 1: Ladder Feymnan graph for non-singlet structure functions. Solid, dashed and wavy lines correspond to quark, photon and gluon, respectively. Crosses mark particles on mass shell.

Fig. 2: Ladder Feynman graphs for singlet structure function for initial gluon (2a) and quark (2b), respectively. Curves are as in Fig. 1. Crosses mark particles on mass shell.

Fig. 3: Non-singlet isovector structure function $f_{1,NS}^{I=1}(x,Q^2)$. a) Dependence of $f_{1,NS}^{I=1}(x,Q^2)$ on x and Q^2. b) Behaviour of logarithmic derivative λ. c) Dependence of ratio R on x and Q^2. Quantities of λ and R are defined in text. Solid, dashed, dotted and dash-dotted lines correspond to $Q^2 = 10$, 30, 100 and 300 (GeV/c)^2, respectively.

Fig. 4: Non-singlet isovector spin-dependent structure function $g_{1,NS}^{I=1}(x,Q^2)$. a) Dependence of $g_{1,NS}^{I=1}(x,Q^2)$ on x and Q^2. b) Behaviour of logarithmic derivative λ. c) Dependence of ratio R on x and Q^2. Quantities of λ and R are defined in text. Curves are as in Fig. 3.

Fig. 5: Non-singlet isoscalar structure function $f_{1,NS}^{I=0}(x,Q^2)$. a) Dependence of $f_{1,NS}^{I=0}(x,Q^2)$ on x and Q^2. b) Behaviour of logarithmic derivative λ. c) Dependence of ratio R on x and Q^2. Quantities of λ and R are defined in text. Curves are as in Fig. 3.

Fig. 6: Non-singlet isoscalar spin-dependent structure function $g_{1,NS}^{I=0}(x,Q^2)$. a) Dependence of $g_{1,NS}^{I=0}(x,Q^2)$ on x and Q^2. b) Behaviour of logarithmic derivative λ. c) Dependence of ratio R on x and Q^2. Quantities of λ and R are defined in text. Curves are as in Fig. 3.

Fig. 7: Singlet gluon spin-dependent structure function $g_{1,S}^{G}(x,Q^2)$ in "ladder" approximation. a) Dependence of $g_{1,S}^{G}(x,Q^2)$ on x and Q^2. b) Behaviour of logarithmic derivative λ. c) Dependence of ratio R_G on x and Q^2. Quantities of λ and R_G are defined in text. Curves are as in Fig. 3.

Fig. 8: Singlet quark spin-dependent structure function $g_{1,S}^{q}(x,Q^2)$ in "ladder" approximation. a) Dependence of $g_{1,S}^{q}(x,Q^2)$ on x and Q^2. b) Behaviour of logarithmic derivative λ. c) Dependence of ratio R_q on x and Q^2. Quantities of λ and R_q are defined in text. Curves are as in Fig. 3.

Fig. 9: Singlet gluon spin-dependent structure function $g_{1,S}^{G}(x,Q^2)$ with effective contributions of non-ladder graphs. a) Dependence of $g_{1,S}^{G}(x,Q^2)$ on x and Q^2. b) Behaviour of logarithmic derivative λ. c) Dependence of ratio R_G^{NL} on x and Q^2. Quantities of λ and R_G^{NL} are defined in text. Curves are as in Fig. 3.

Fig. 10: Singlet quark spin-dependent structure function $g_{1,S}^{q}(x,Q^2)$ with effective contributions of non-ladder graphs. a) Dependence of $g_{1,S}^{q}(x,Q^2)$ on x and Q^2. b) Behaviour of logarithmic derivative λ. c) Dependence of ratio R_q^{NL} on x and Q^2. Quantities of λ and R_q^{NL} are defined in text. Curves are as in Fig. 3.

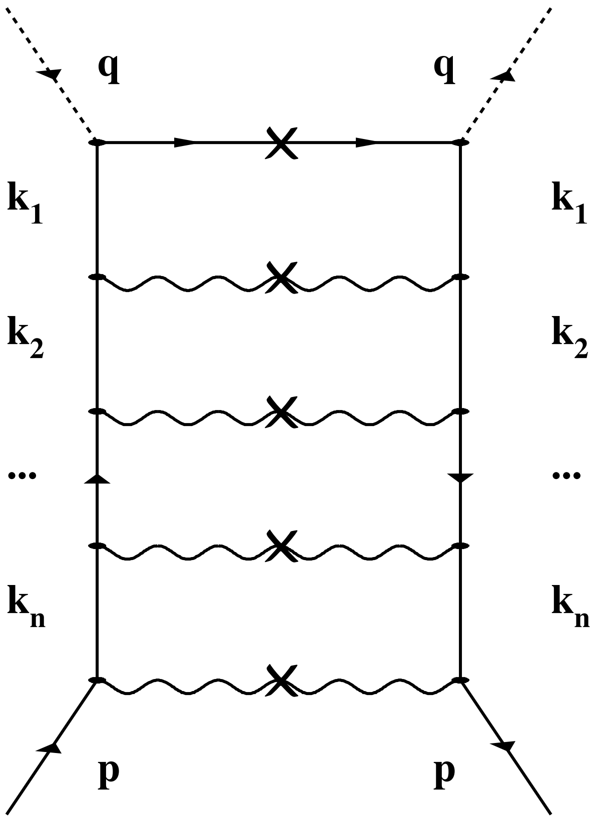
q
q
k_1
k_1
k_2
k_2
...
...
k_n
k_n
p
p

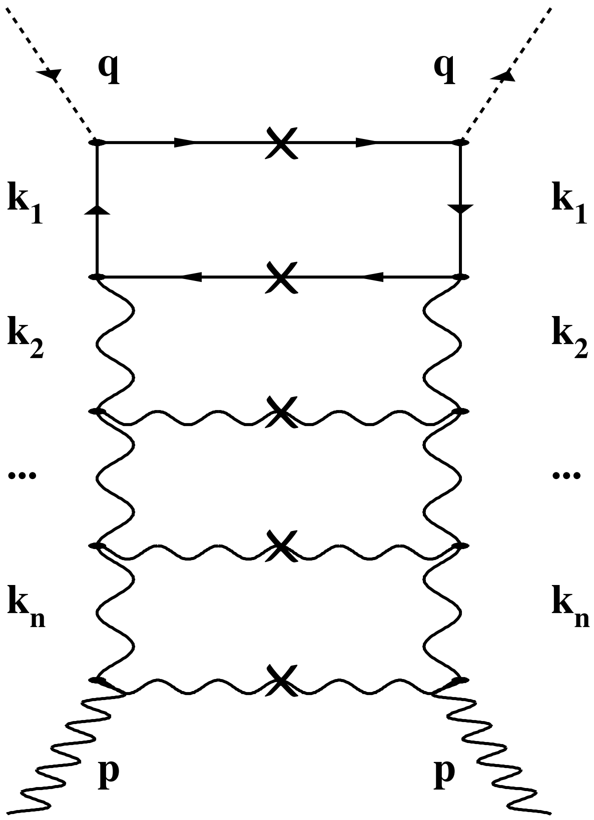
q
q
k1
k1
k2
k2
...
...
kn
kn
p
p

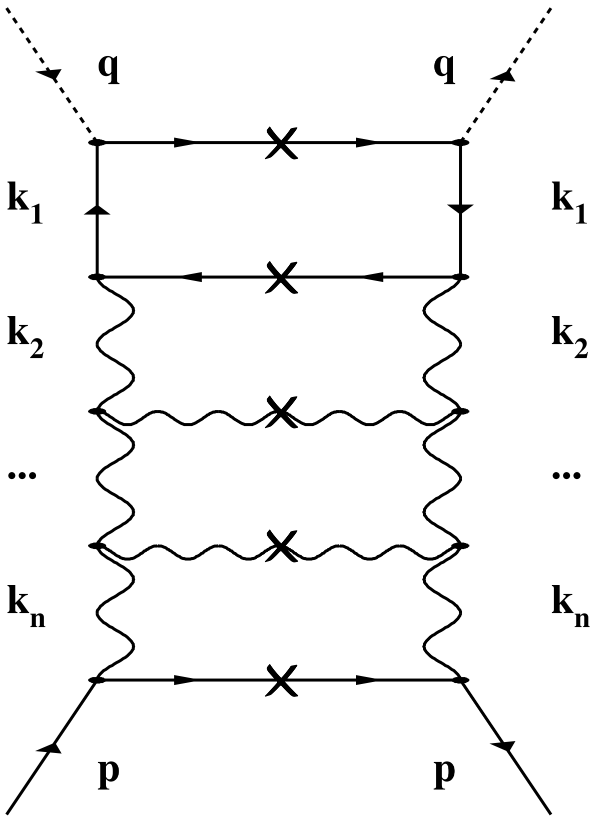
q
q
k1
k1
k2
k2
...
...
kn
kn
p
p

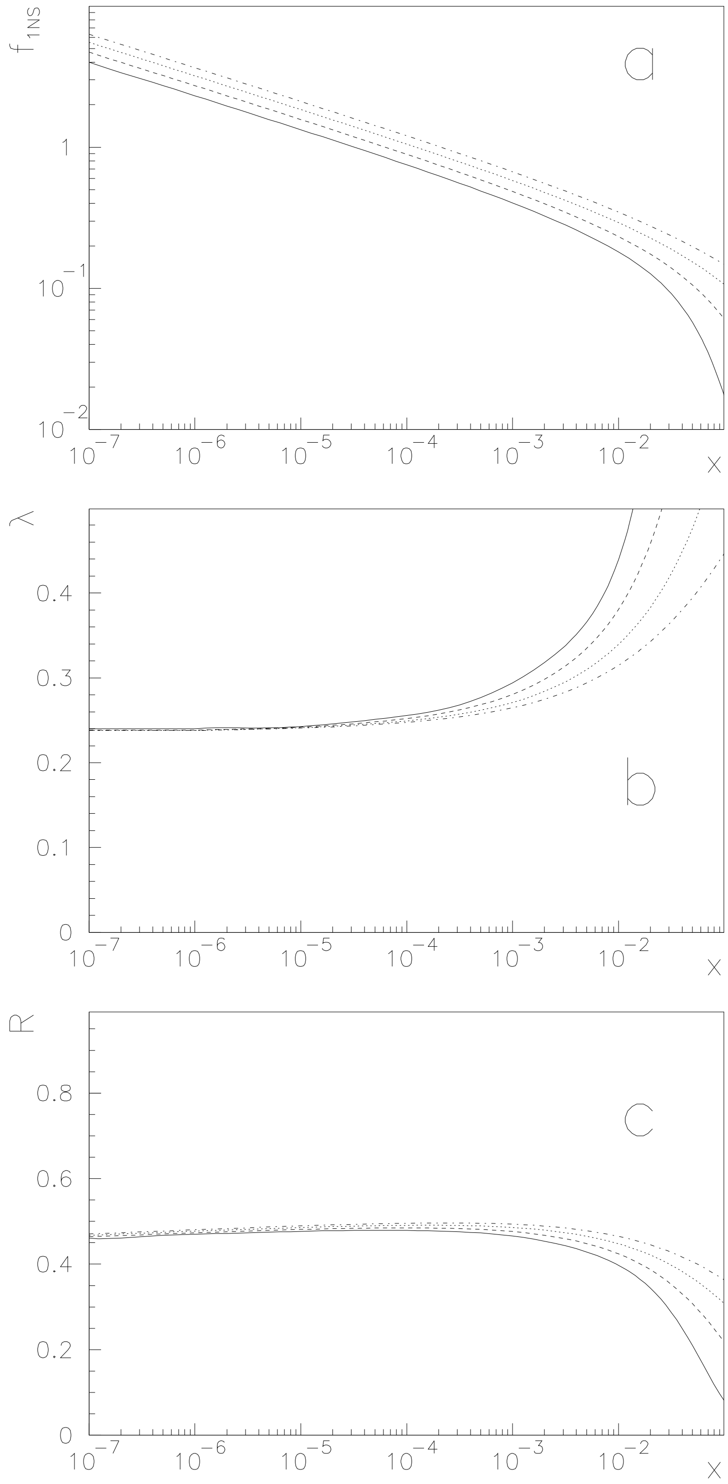

f_1NS
a
1
10^-1
10^-2
10^-7 10^-6 10^-5 10^-4 10^-3 10^-2
x
λ
0.4
0.3
0.2
0.1
0
b
R
0.8
0.6
0.4
0.2
c

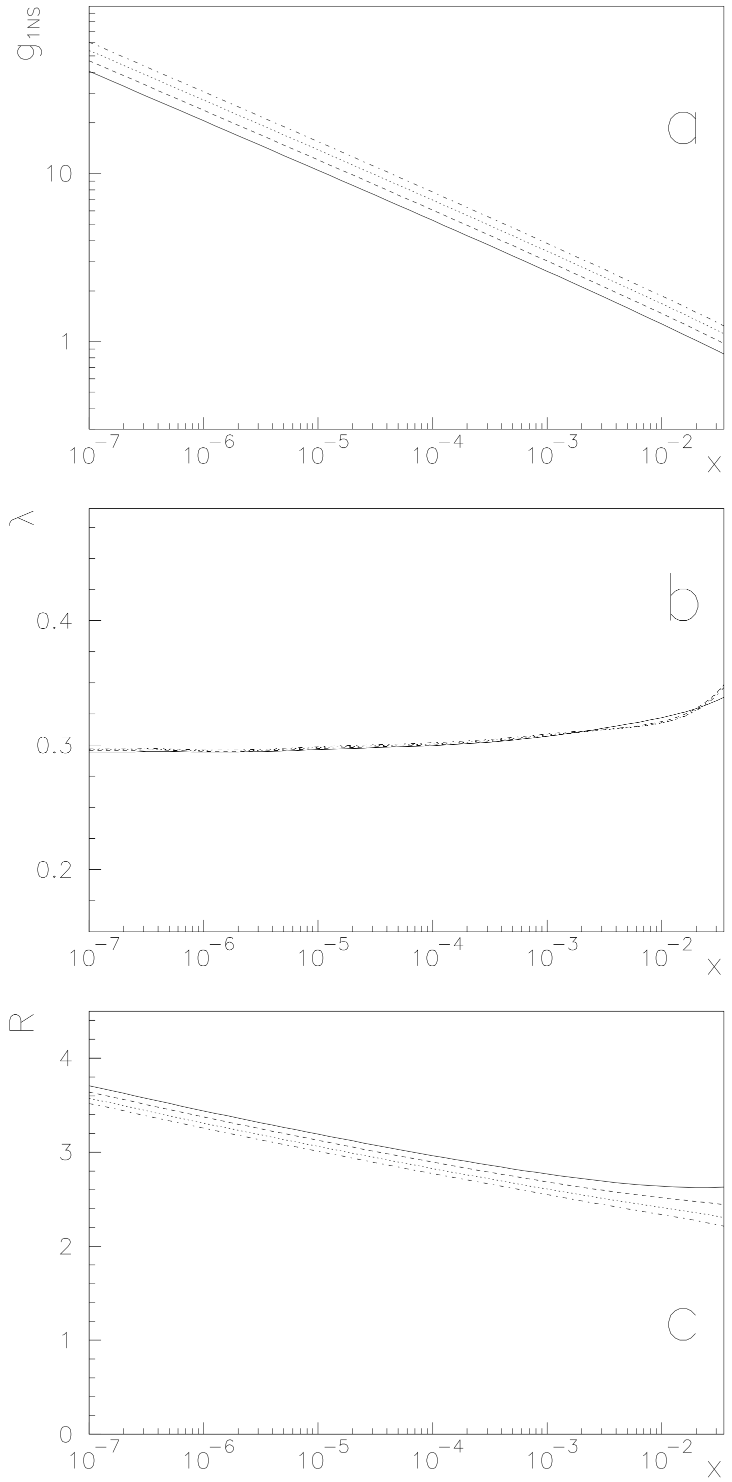

g1NS
a
10
1
λ
b
0.4
0.3
0.2
R
c
4
3
2
1
0
10−7
10−6
10−5
10−4
10−3
10−2
x

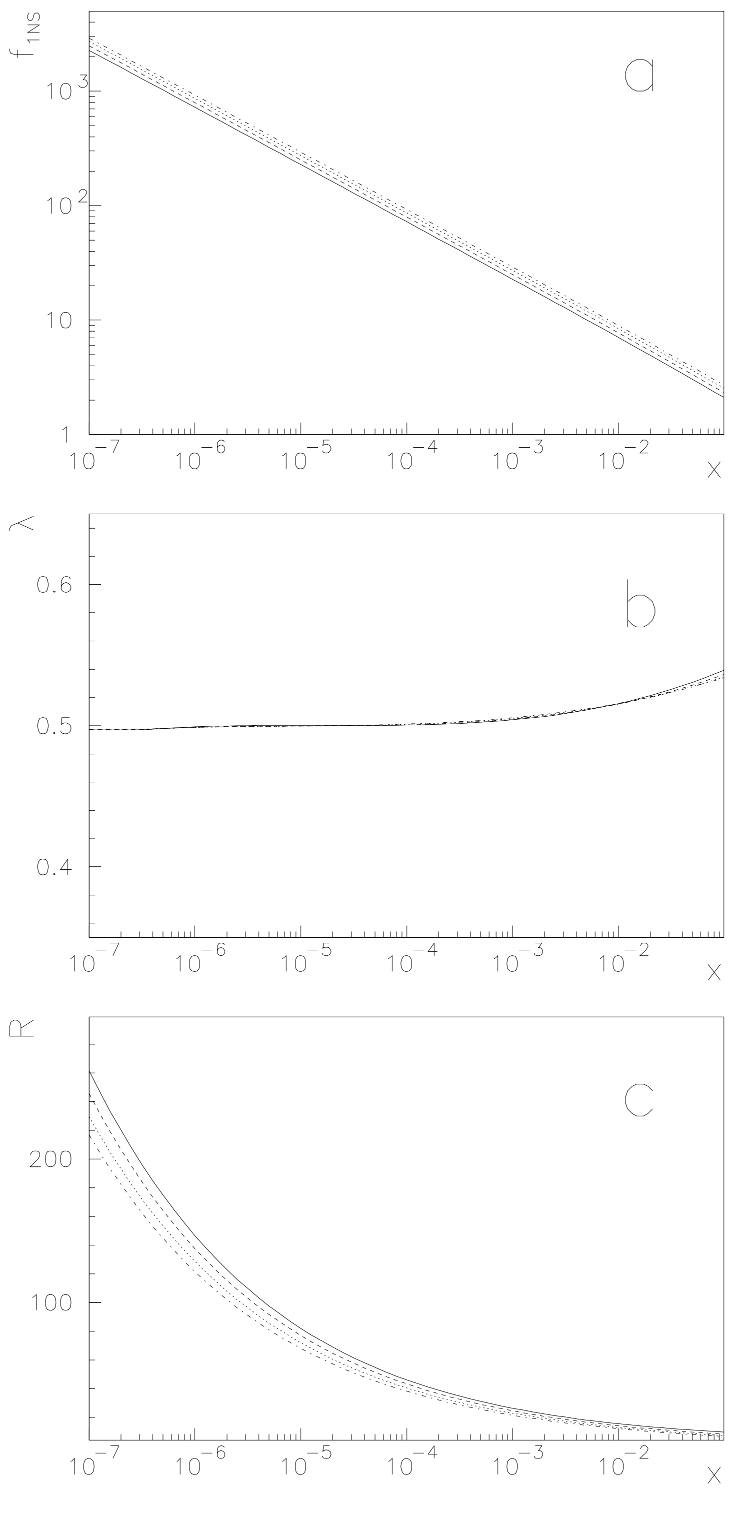
f_1NS
a
10^3
10^2
10
1
10^-7 10^-6 10^-5 10^-4 10^-3 10^-2
x
λ
b
0.6
0.5
0.4
10^-7 10^-6 10^-5 10^-4 10^-3 10^-2
x
R
c
200
100
10^-7 10^-6 10^-5 10^-4 10^-3 10^-2
x

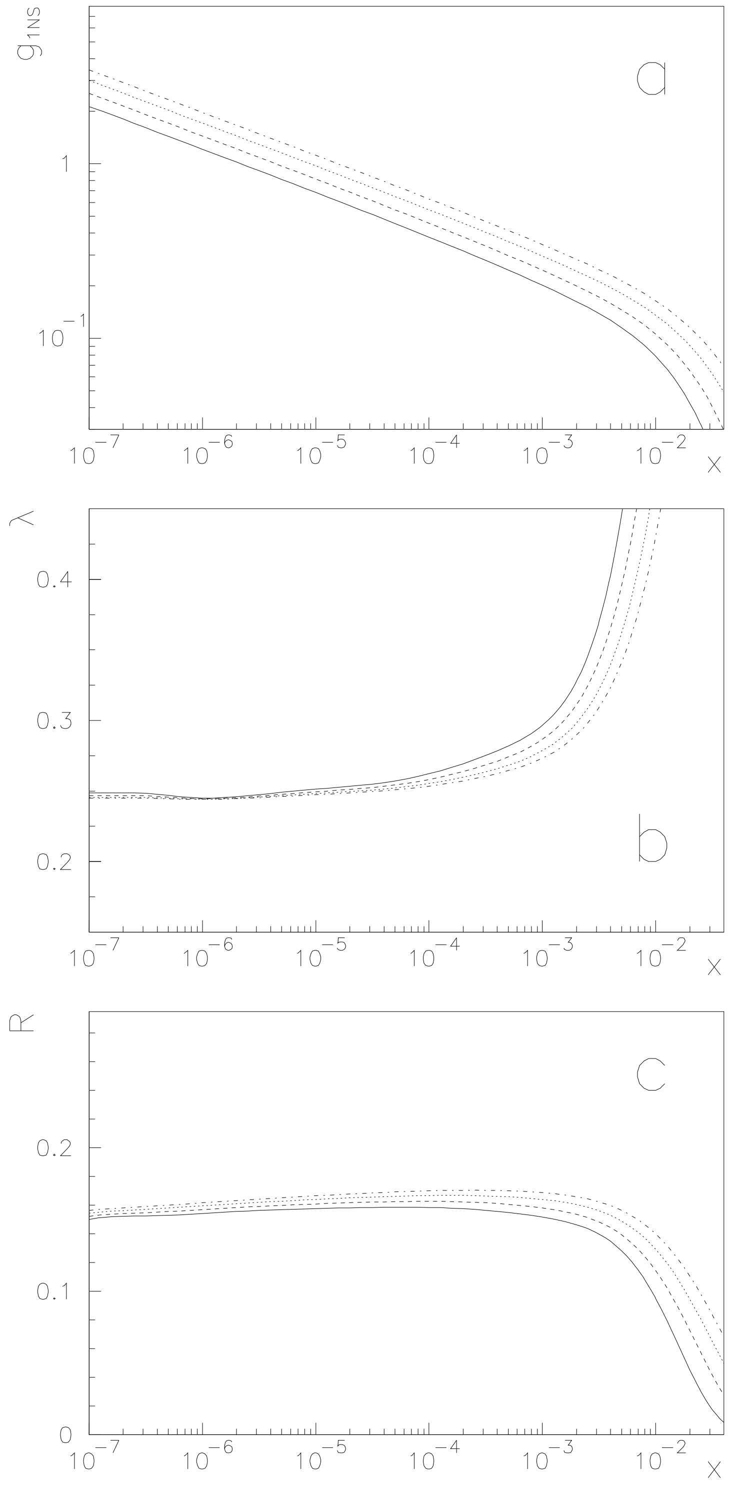

g_{1NS}
a
1
10^{-1}
10^{-7} 10^{-6} 10^{-5} 10^{-4} 10^{-3} 10^{-2}
x
λ
0.4
0.3
0.2
b
10^{-7} 10^{-6} 10^{-5} 10^{-4} 10^{-3} 10^{-2}
x
R
c
0.2
0.1
0
10^{-7} 10^{-6} 10^{-5} 10^{-4} 10^{-3} 10^{-2}
x

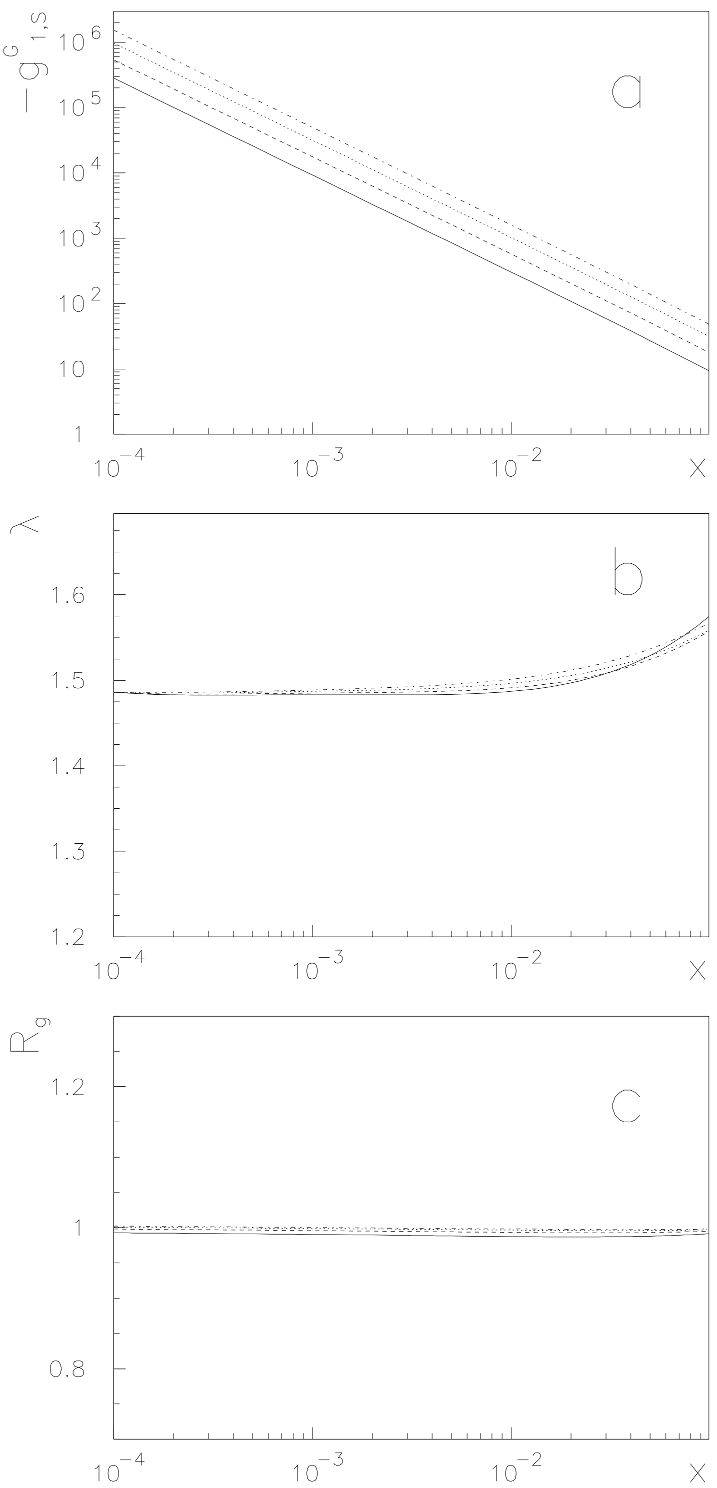

$-g^G_{1,s}$
a
λ
b
R_g
c
X

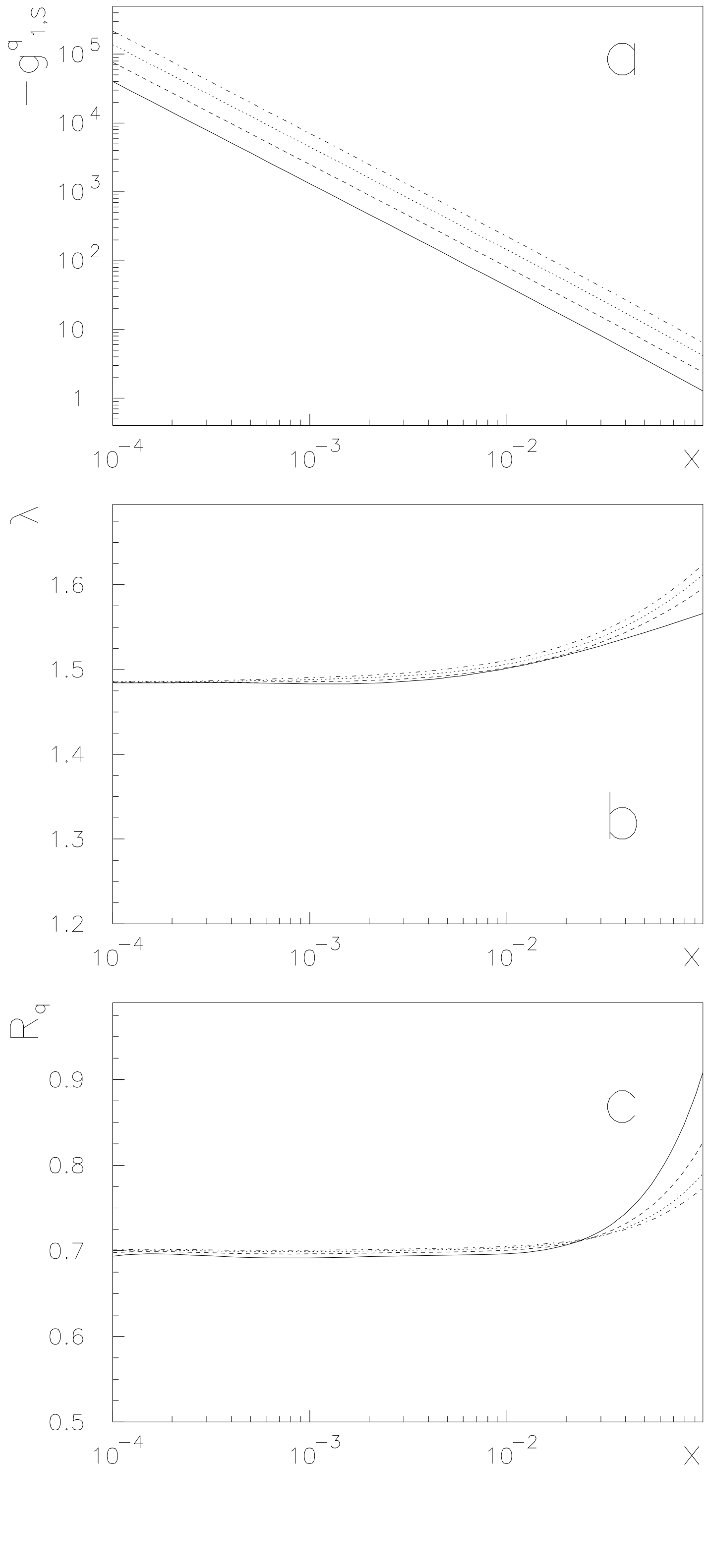

$-g^q_{1,s}$
10^5
10^4
10^3
10^2
10
1
a
10^{-4}
10^{-3}
10^{-2}
x
λ
1.6
1.5
1.4
1.3
1.2
b
10^{-4}
10^{-3}
10^{-2}
x
R_q
0.9
0.8
0.7
0.6
0.5
c
10^{-4}
10^{-3}
10^{-2}
x

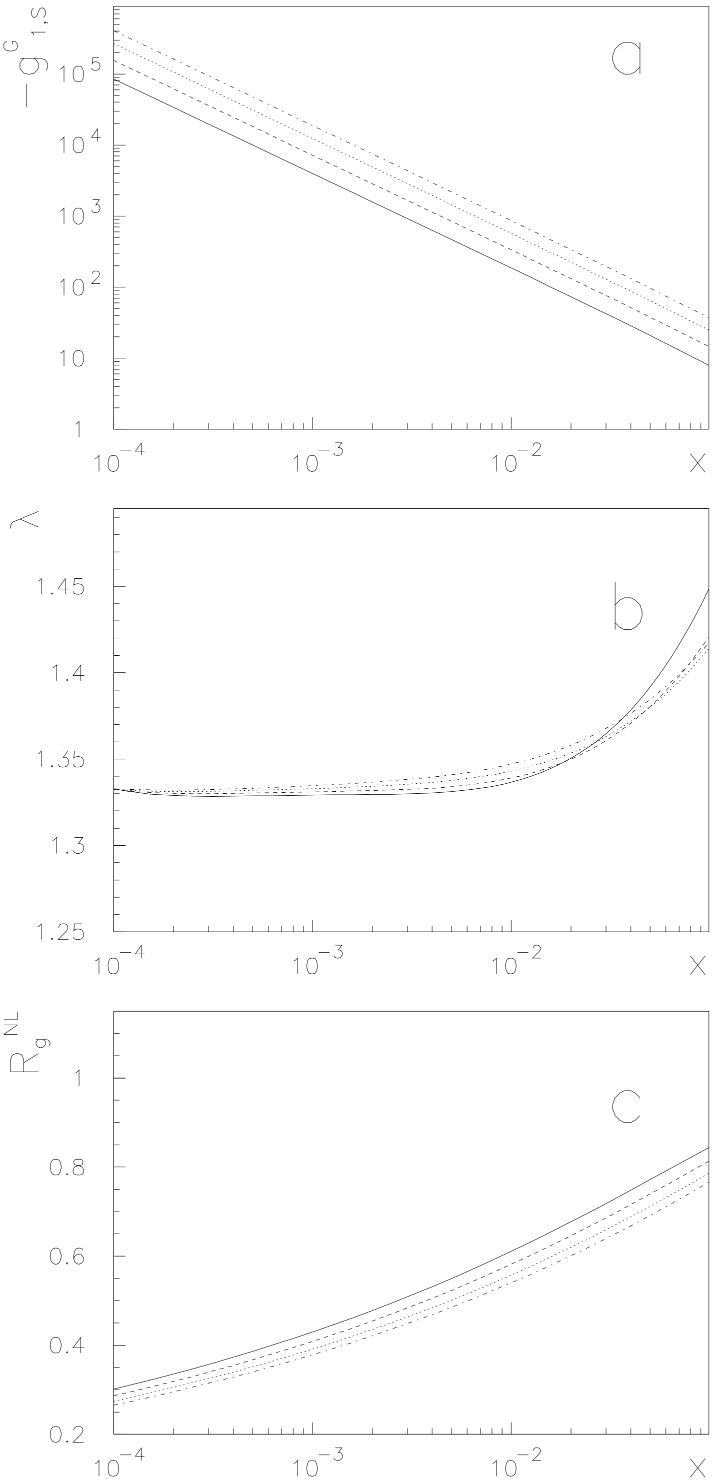

$-g^G_{1,S}$
a
10^5
10^4
10^3
10^2
10
1
10^{-4}
10^{-3}
10^{-2}
X
λ
b
1.45
1.4
1.35
1.3
1.25
10^{-4}
10^{-3}
10^{-2}
X
R_g^{NL}
c
1
0.8
0.6
0.4
0.2
10^{-4}
10^{-3}
10^{-2}
X

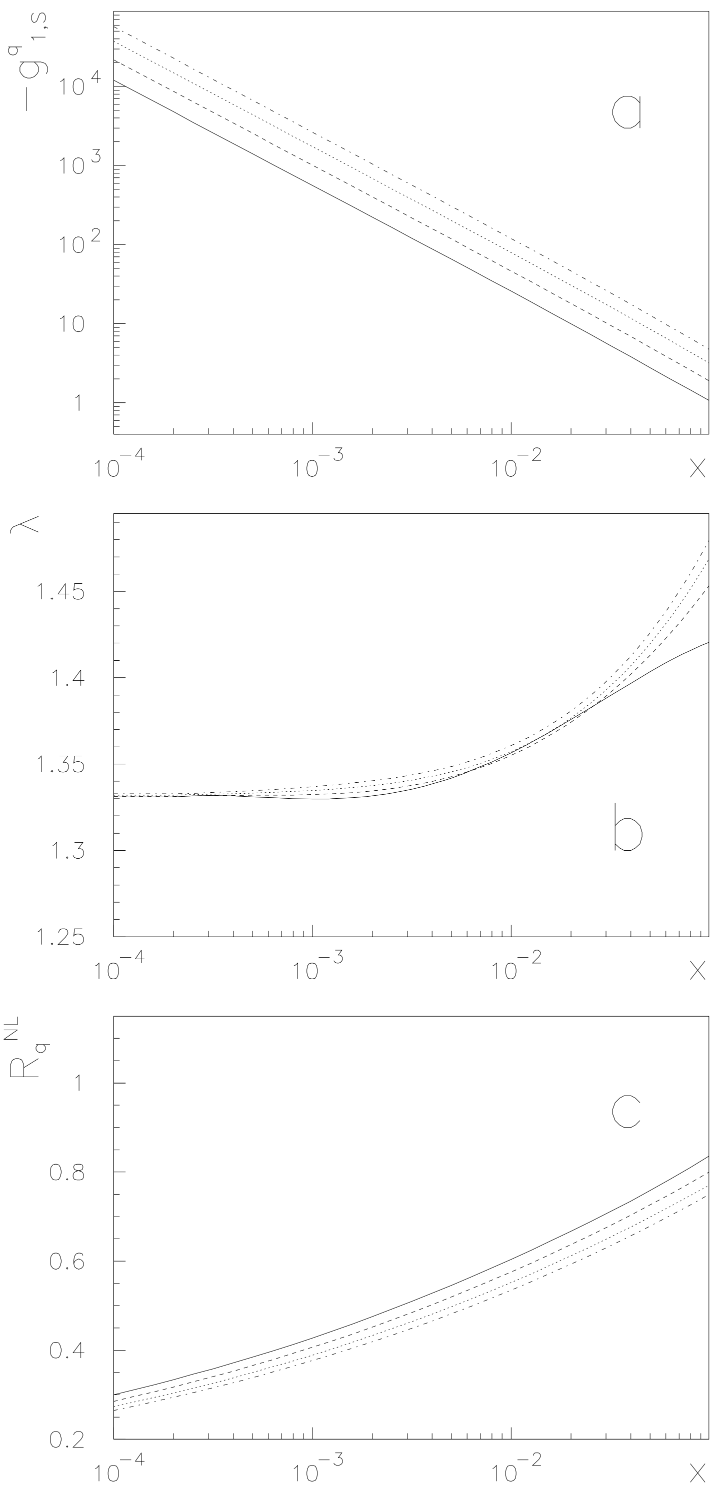

$-g^q_{1,S}$
10^4
10^3
10^2
10
1
a
10^{-4}
10^{-3}
10^{-2}
X
λ
1.45
1.4
1.35
1.3
1.25
b
R_q^{NL}
1
0.8
0.6
0.4
0.2
c